

A Novel Technique for Studying the Z Boson Transverse Momentum Distribution at Hadron Colliders

M. Vesterinen, T. R. Wyatt.

Particle Physics Group, School of Physics and Astronomy, University of Manchester, UK.

Abstract

We present a novel method for studying the shape of the Z boson transverse momentum distribution, Q_T , at hadron colliders in $p\bar{p}/pp \rightarrow Z/\gamma^* \rightarrow l^+l^-$. The Q_T is decomposed into two orthogonal components; one transverse and the other parallel to the di-lepton thrust axis. We show that the transverse component is almost insensitive to the momentum resolution of the individual leptons and is thus more precisely determined on an event-by-event basis than the Q_T . Furthermore, we demonstrate that a measurement of the distribution of this transverse component is substantially less sensitive to the dominant experimental systematics (resolution unfolding and Q_T dependence of event selection efficiencies) reported in previous measurements of the Q_T distribution.

Key words:

PACS: 12.38.Qk, 13.85.Qk, 14.70.Hp, 12.38.Lg, 12.15.Mm

1 Introduction

The shape of the Z boson momentum distribution transverse to the beam direction (Q_T) at a hadron collider tests the predictions of quantum chromodynamics (QCD), since non-zero Q_T is generated through radiation from the initial state partons. A good understanding of electroweak vector boson production is important in precision measurements (e.g. top quark and W boson mass) and in Higgs boson and new phenomena searches at hadron collider experiments. In many of these searches the signal and/or background processes involve electroweak vector bosons produced in association with jets.

At low Q_T ($Q_T \ll Q$), where the emission of multiple soft gluons is important, calculations in fixed order perturbative QCD diverge. There exist resummation techniques, in which singular contributions from all orders of α_s are resummed to give a finite result. Resummation was first applied to the Drell-Yan process by Collins, Soper and Sterman (CSS) [1]. The resummation is carried out in impact parameter (b) space and includes a non-perturbative (NP) form factor that needs to be determined from data. Brock, Landry, Nadolsky and Yuan (BLNY) proposed the following parameterisation [2]:

$$S_{NP}(b, Q^2) = \left[g_1 + g_2 \ln \left(\frac{Q}{2Q_0} \right) + g_1 g_3 \ln(100x_i x_j) \right] b^2 \quad (1)$$

where x_i and x_j are the fractions of the hadron momenta carried by the initial state partons, Q_0 is an arbitrary scale set to 1.6 GeV and the parameters g_i need to be fitted from data.

Using the BLNY NP form factor, the CSS formalism was able to describe simultaneously Tevatron Run I Z data and lower Q^2 Drell-Yan data in a global fit of the parameters g_i [2]. The Q_T distribution at the Tevatron ($Q^2 \sim M_Z^2$) is sensitive to g_2 and insensitive to g_1 and g_3 . A larger value of g_2 corresponds to a harder Q_T distribution. The CSS formalism is implemented in the next to leading order (NLO) event generator ResBos [3]. In Run II the DØ Collaboration reported a Q_T measurement in the di-electron channel with 1 fb^{-1} of data [4]. For low Q_T ($Q_T < 30 \text{ GeV}$), the DØ data is, within the measurement uncertainties, well described by the CSS/BLNY formalism.

At low Q_T the overall uncertainties were dominated by the parton distribution functions (PDFs) and the following experimental systematics [4]:

- Unfolding the Q_T measurement to account for the resolution in the measurement of the E_T of the electrons.
- Correcting for the Q_T dependence of the overall event selection efficiency.

As a result of these substantial experimental systematics, the low Q_T region was not much better measured in this 1 fb^{-1} Run II analysis than in the 100 pb^{-1} Run I analysis [5]. In both analyses, a measurement was made of g_2 . The measurements: $0.59 \pm 0.06 \text{ GeV}^2$ for Run I and $0.77 \pm 0.06 \text{ GeV}^2$ for Run II, have comparable uncertainties ¹.

An observable that is sensitive to the Q_T , but less sensitive to these experi-

¹ The DØ Run I and Run II measurements cannot be directly compared since they used different PDFs and the Run I measurement used the the Ladinsky-Yuan (LY) parameterisation [15] of the NP form factor as opposed to the BLNY parameterisation. Only the third term in $g_1 g_3$ is different and any shift in the fitted g_2 is far smaller than the uncertainties on these measurements.

mental systematics would be beneficial. In this work, Monte Carlo studies of an optimal observable, a_T , are presented. The a_T observable has previously been used in the selection of $l^-l^+\nu\bar{\nu}$ final states at LEP by the OPAL collaboration [6]. The UA2 Collaboration used a similar observable, p_η^Z , which we refer to as b_T , in a Q_T measurement [7].

2 Constructing the Observable

The measured Q_T is highly sensitive to the lepton p_T resolution. Our goal is to build an observable that is less sensitive to this resolution, whilst still sensitive to the Q_T . We keep in mind the fact that collider detectors generally have far better angular resolution than calorimeter E_T or track p_T resolution.

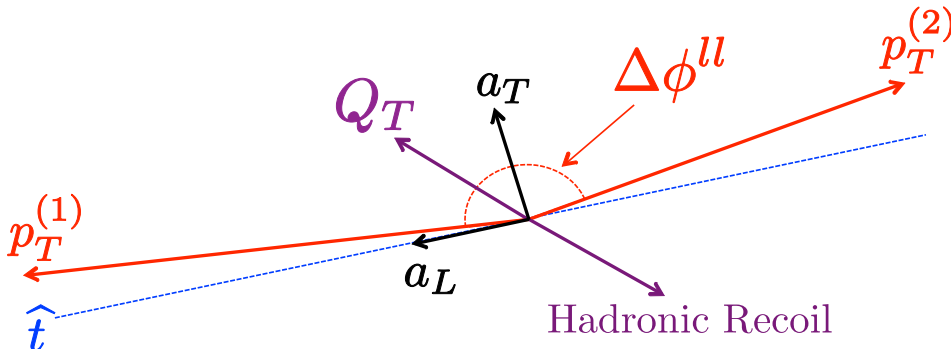


Fig. 1. A schematic representation in the transverse plane, of the construction of a_T and a_L in a typical leptonic Z decay. The hadronic recoil is expected to have equal and opposite transverse momentum to the Z .

For events with di-lepton azimuthal separation, $\Delta\phi^{ll} > \frac{\pi}{2}$, the Q_T is decomposed into orthogonal components as follows (See figure 1):

- The thrust axis is defined as: $\hat{t} = \frac{\vec{p}_T^{(1)} - \vec{p}_T^{(2)}}{|\vec{p}_T^{(1)} - \vec{p}_T^{(2)}|}$ where $\vec{p}_T^{(i)}$ is the transverse momentum vector of lepton i . The two leptons have equal momentum transverse to this axis.
- The transverse momentum vector of the di-lepton system, $\vec{Q}_T = \vec{p}_T^{(1)} + \vec{p}_T^{(2)}$, is decomposed into components transverse to the axis, $a_T = |\vec{Q}_T \times \hat{t}|$, and aligned with the axis, $a_L = \vec{Q}_T \cdot \hat{t}$.

For events with $\Delta\phi^{ll} < \frac{\pi}{2}$, a_T is set equal to the Q_T , while a_L maintains the same definition for all values of $\Delta\phi^{ll}$.

At low Q_T , $\Delta\phi^{ll} \sim \pi$, hence the uncertainty on a_T is approximately the uncertainty on the individual lepton p_T 's multiplied by the sine of a small angle. In contrast, the uncertainty on a_L (and thus also Q_T) is approximately

the uncertainty on the individual lepton p_T 's multiplied by the cosine of a small angle.

An alternative observable is discussed, b_T , whose construction is identical to that of a_T except that the decomposition is performed relative to the di-lepton perpendicular bisector axis: $\hat{b} = \frac{\vec{p}_T^{(1)} - r\vec{p}_T^{(2)}}{|\vec{p}_T^{(1)} - r\vec{p}_T^{(2)}|}$ where $r = |\vec{p}_T^{(1)}|/|\vec{p}_T^{(2)}|$. The two leptons have equal acoplanarity with respect to this axis. In an event in which the leptons have equal p_T , the values of a_T and b_T are equal. No study is presented of the component longitudinal to the axis, b_L .

As discussed below, the relative sensitivity to lepton p_T mis-measurement of a_T and b_T depends on the correlation between the lepton p_T and its resolution.

3 Monte Carlo Simulation

Monte Carlo (MC) events are generated using PYTHIA [8], which treats at leading order (LO) the process $p\bar{p} \rightarrow Z/\gamma^* \rightarrow \mu^+\mu^-$ plus up to one jet, at a centre of mass energy of 1.96 TeV, and mass between 60 and 130 GeV. PYTHIA uses additional parton showering to simulate “soft” transverse momentum generation. Although this study is carried out with $Z \rightarrow \mu^+\mu^-$ events, the idea is applicable to studying the di-electron channel.

In order to simulate the imperfect muon p_T resolution of a detector, Gaussian smearing of width 0.003 GeV^{-1} is applied in $1/p_T$ to both muons, which is approximately the design muon p_T resolution of the Run II DØ detector [9]. The design tracking resolution of other current and future hadron collider detectors; CDF, ATLAS and CMS [10,11,12] vary between $\approx 10^{-3}$ and $\approx 10^{-4} \text{ GeV}^{-1}$ depending on the track p_T and pseudo-rapidity (η). We refer to the constant $\delta(1/p_T)$ form of the resolution p_T dependence as *muon-like*. An alternative resolution dependence is studied; *electron-like* resolution with the form: $\delta p_T/p_T = 0.15/p^{1/2}$, which would be the form expected for a calorimeter-based measurement appropriate for electrons. Gaussian smearing is applied to the lepton azimuthal angle ϕ of width 0.0005 rad., which is the typical resolution of a detector.

In order to study the dependence of event selection efficiency on Q_T , a_T , a_L and b_T , the following simple cuts are applied to the event sample. These are representative of the cuts typically applied to select Z decays at a hadron collider.

- The di-muon invariant mass must be between 70 and 110 GeV.
- Kinematic cuts on both muons: $p_T > 15 \text{ GeV}$ and $|\eta| < 2$.

- An isolation cut on both muons: $f_{iso} < 2.5$ GeV, where $f_{iso} = \sum p_T(\Delta R < 0.2)$ and $\Delta R = \sqrt{(\Delta\eta)^2 + (\Delta\phi)^2}$ is the radius of a cone around the candidate muon. The sum is over all particles excluding both the candidate muon and any neutrinos.

PYTHIA is a LO event generator and is not expected to give a good description of the Q_T distribution in real data. The events are re-weighted in Q_T and Z rapidity (y) to match the prediction of ResBos using the default settings, which is in good agreement with $D\bar{O}$ Run II data [4] in the region of low Q_T ($Q_T < 40$ GeV). Event samples are generated using ResBos, and the re-weighting procedure is carried out as follows:

- Two dimensional histograms in Q_T and $|y|$ are produced for both the PYTHIA and ResBos event samples.
- Dividing the ResBos histogram by the PYTHIA histogram gives an *event-weight* histogram.
- The PYTHIA events are now given an *event-weight* based on their Q_T and $|y|$ such that the distributions of these variables are the same as the ResBos prediction.

Hereafter, unless otherwise stated, MC refers to PYTHIA re-weighted to ResBos.

4 Sensitivity to Lepton p_T Mis-measurement

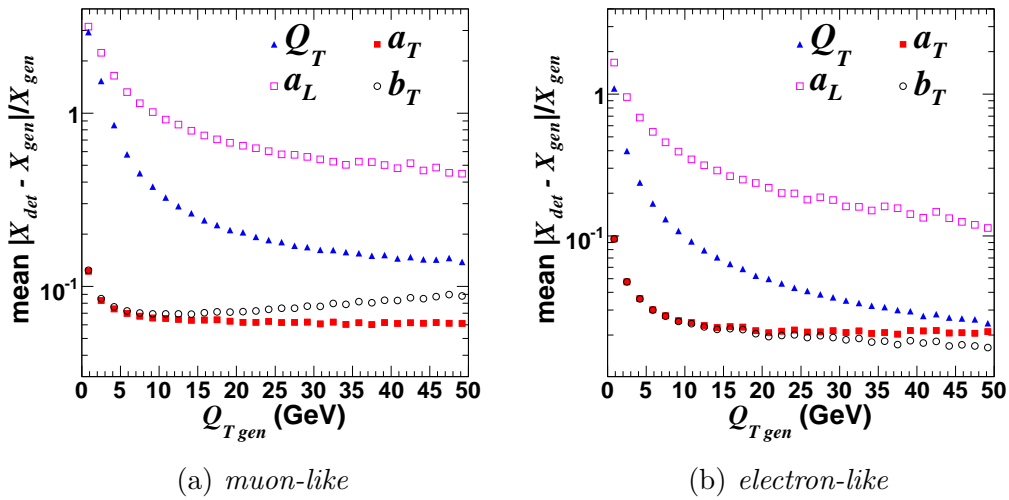


Fig. 2. Mean resolution, $|X_{det} - X_{gen}|/X_{gen}$ for each of the observables, Q_T , a_T , a_L and b_T as a function of Q_{Tgen} , with (a) *muon-like* resolution ($\delta(1/p_T) = 0.003$ GeV $^{-1}$) and (b) *electron-like* resolution ($\delta p_T/p_T = 0.15/p^{1/2}$).

Two quantities are defined: the smeared or *detector level* quantity, X_{det} , and the unsmeared or *generator level* quantity, X_{gen} , where X corresponds to Q_T , a_T , a_L or b_T .

Figures 2 (a) and 2 (b) show the mean resolution, $|X_{det} - X_{gen}|/X_{gen}$ as a function of Q_{Tgen} for *muon-like* and *electron-like* resolution respectively. It can be seen that for low to moderate values of Q_T ($Q_{Tgen} < 50$ GeV), a_T and b_T are significantly better measured than a_L or Q_T . Either a_T or b_T are therefore particularly well suited to studying Z production at low to moderate Q_T . In the region of low Q_T ($Q_{Tgen} < 15$ GeV), a_T and b_T have similar resolutions for either the (a) *muon-like* or (b) *electron-like* cases. At increasing Q_T , a_T is more suited for (a), and b_T more suited for (b). The construction of a_T ensures that the acoplanarity angle to the thrust axis is smaller for the larger p_T lepton which tends to have poorer resolution in the *muon-like* case. In the following sections, for brevity, we discuss the case of *muon-like* smearing.

5 Event Selection Efficiency Dependence

Figure 3 shows the dependence of the event selection efficiency (separately for the cuts on muon $|\eta|$, p_T and isolation) on the generator level Q_T , a_T , a_L and b_T . The cuts are applied in the following order: $|\eta|$; p_T ; isolation. The efficiency dependence for each cut is calculated having applied all previous cuts. For large Q_T , the muons tend to be more central, increasing the η cut efficiency. The same correlation is apparent for a_T and a_L , although weaker than for Q_T .

The muon p_T cut dependence on a_T is flat in the range considered. Conversely large values of a_L , generate an asymmetry in the p_T 's of the two muons and tend to push the lower p_T muon below the cut threshold. The dependence on the isolation cut is substantially flatter for a_T than for a_L . Large a_L corresponds to a high p_T hadronic recoil with a large fraction of its p_T aligned along the thrust axis and thus possibly lying within the isolation cone of one of the two muons. There is no such dependence on a_T , since a_T is the component of the recoil p_T transverse to the thrust axis.

In summary, the efficiencies of the cuts on muon $|\eta|$, p_T and isolation depend less strongly on a_T than Q_T . The dependence of b_T on each of the cuts is similar to that of a_T .

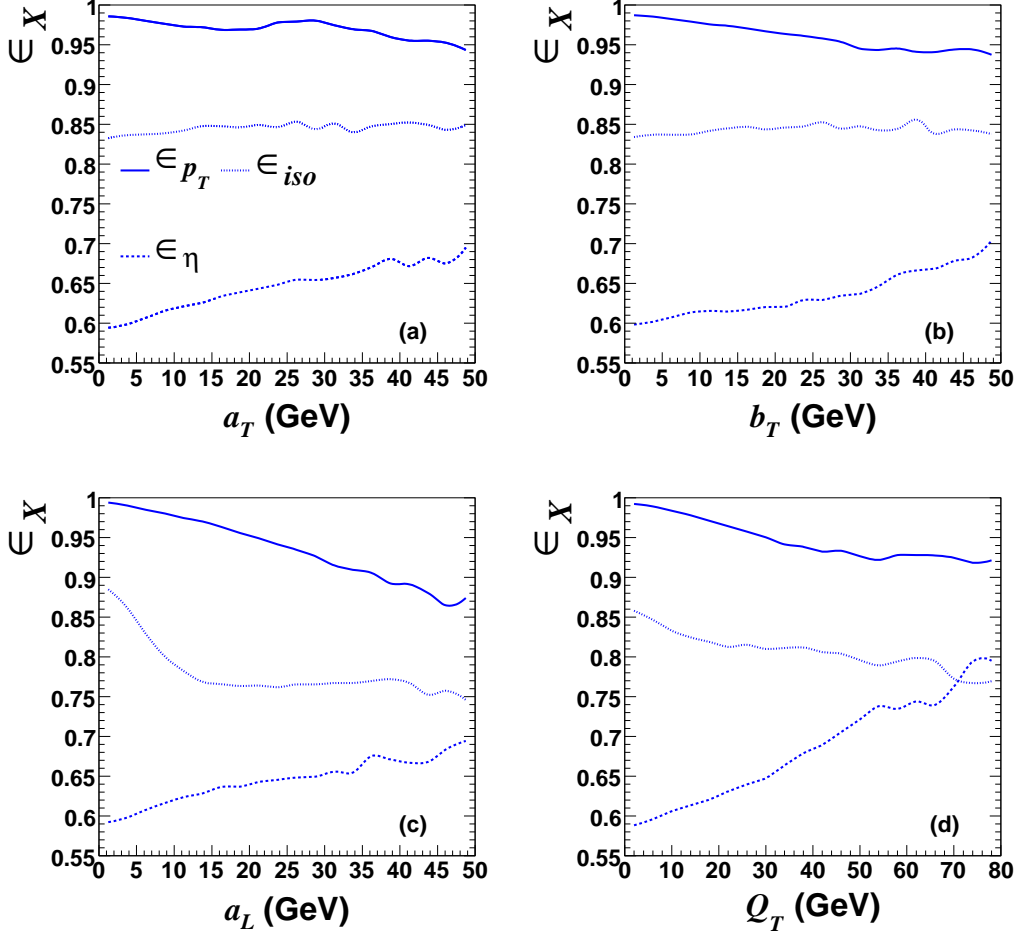


Fig. 3. The dependence of event selection efficiencies on the generator level (a) a_T , (b) b_T , (c) a_L and (d) Q_T in $Z \rightarrow \mu^+ \mu^-$ MC events. The efficiencies ϵ_{η} , ϵ_{p_T} and ϵ_{iso} (evaluated relative to the previous cut in the order; $|\eta|$, p_T , isolation) are shown separately for cuts on muon $|\eta|$, p_T and isolation respectively. Note that the range of Q_T shown in this figure is $\sqrt{2} \times$ larger than for a_T and a_L .

6 Systematic Uncertainties on the Unfolded and Efficiency Corrected Distributions

Figure 4 compares (separately for Q_T , a_T , a_L and b_T) the *generator level* distributions *without* selection cuts and the *detector level* distributions *with* selection cuts. The detector level Q_T and a_L distributions are substantially affected by the detector resolution and event selection efficiency. In contrast the distributions in a_T and b_T are almost completely unaffected.

In order to extract the underlying shape, the measured distributions would need to be unfolded for the detector resolution and corrected for the event selection efficiency with associated systematic uncertainties. These uncertain-

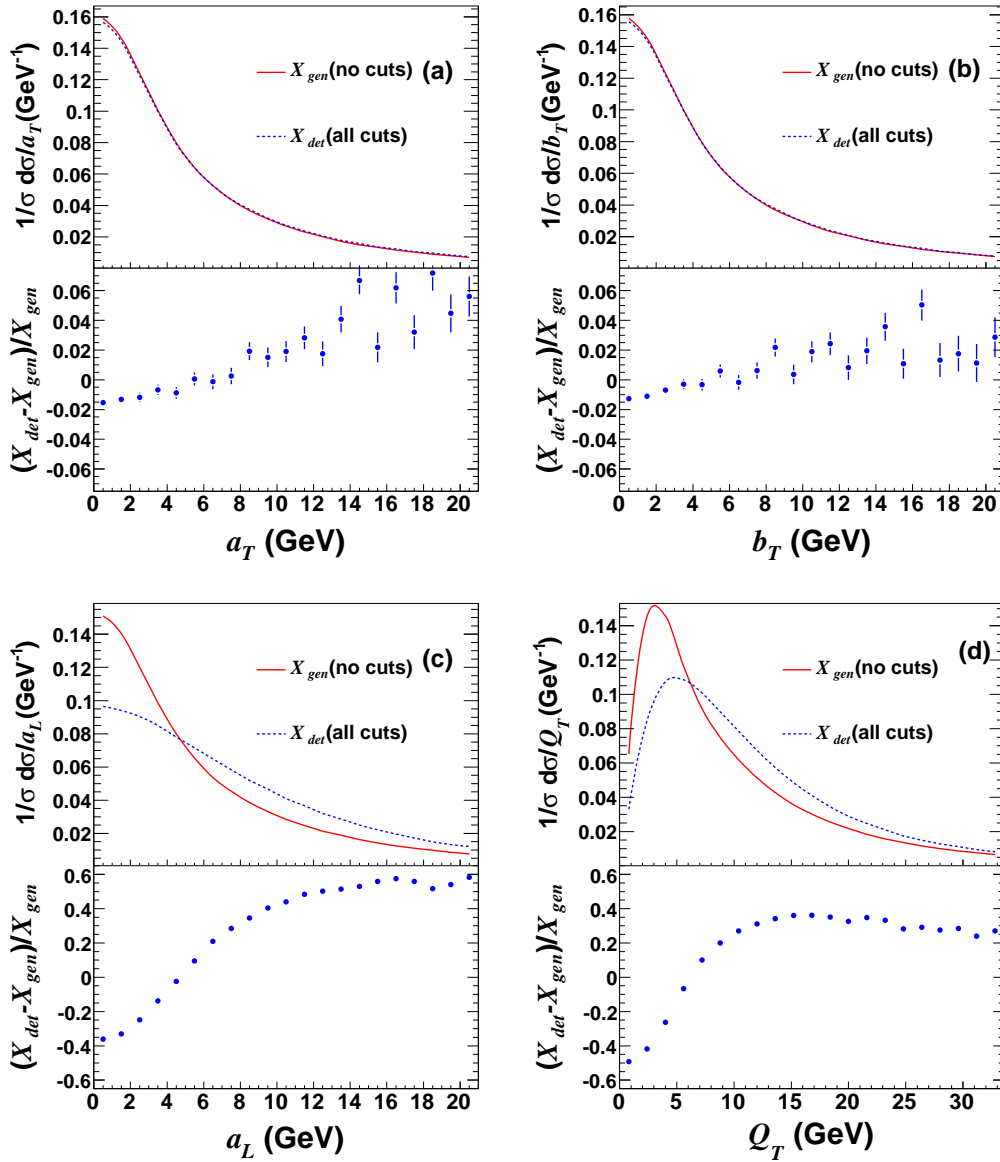


Fig. 4. Detector and generator level distributions for (a) a_T , (b) b_T , (c) a_L and (d) Q_T . The detector level distributions are for Gaussian smearing in $1/p_T$ of width 0.003 GeV^{-1} , and all selection cuts are applied. The generator level distributions do not include selection cuts. The lower halves of each plot show the fractional differences.

ties would be substantially smaller for a_T or b_T than for Q_T or a_L . In fact, for any realistic detector resolution, the measured a_T or b_T distribution describes the underlying distribution within a few percent without any unfolding or efficiency correction at all. The statistical sensitivity of a_T or b_T to the shape of the underlying Q_T distribution is also enhanced by the lack of resolution smearing compared to Q_T .

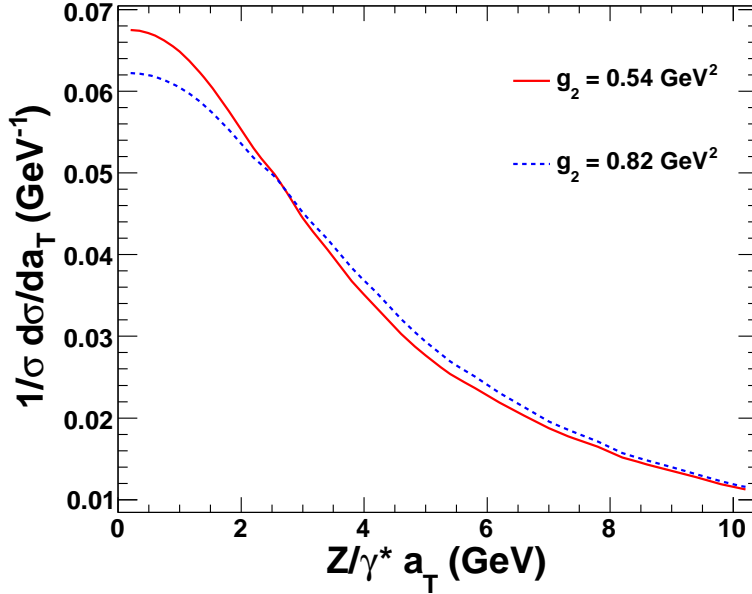


Fig. 5. The generator level prediction of the a_T distribution of PYTHIA (re-weighted to ResBos) for two different g_2 values.

7 Uncertainties in Measurements of NP Phenomenological Parameters

In a “toy” MC measurement of the BLNY parameter g_2 , we study both the sensitivity to systematic uncertainties and the statistical sensitivity of a_T , a_L , Q_T and b_T . Figure 5 shows the PYTHIA (re-weighted to ResBos) prediction of the normalized a_T distribution for two different values of g_2 . The a_T distribution is clearly sensitive to the value of g_2 .

Event samples are generated using ResBos, for fifteen g_2 values from 0.54 to 0.82 (distributed around the world average, $g_2 = 0.68^{+0.02}_{-0.01} \text{ GeV}^2$) [2]. Using the re-weighting procedure described earlier, PYTHIA “MC samples” are produced corresponding to each of the g_2 values. An independent sample of 200k PYTHIA events is re-weighted to the central g_2 value and represents the experimental “pseudo-data” sample.

For each of the 15 MC templates, the pseudo-data vs MC χ^2 is calculated. The function: $y = a(x - b)^2 + c$ is fitted to the χ^2 as a function of g_2 , and a best fit g_2 is determined as $b \pm a^{-1/2}$ where the uncertainty is statistical ($\Delta\chi^2 = \pm 1$).

This “toy” measurement of g_2 serves as an example analysis at an experiment. Free parameters in any NP model which affect the Q_T could in principle be measured using this strategy.

7.1 Systematic Uncertainties

We study the systematic uncertainties on a fit to g_2 . The following systematic variations are carried out. These are typical of the experimental uncertainties expected at a hadron collider although the size of the variations are chosen to give reasonable shifts in the fitted g_2 :

- In the MC, the smearing constant ($\delta(1/p_T)$) is varied by a factor $\pm 1\%$ around a central value of 0.003 GeV^{-1} .
- As a test of sensitivity to mis-measurement of the event selection efficiency dependencies on, $|\eta|$, p_T and isolation, events in MC are given $\pm 10\%$ more weight for each muon with; $1 < |\eta| < 2$, $15 < p_T < 20 \text{ GeV}$, or $1 < f_{iso} < 2.5 \text{ GeV}$.
- In the MC, the ϕ smearing constant is varied by $\pm 10\%$.
- As a test of sensitivity to mis-modeling of final state radiation (FSR), events in MC are given $\pm 10\%$ more weight if the difference between the generator level Z mass and the generator level di-lepton mass is greater than 1 GeV .

Table 1

The shifts (%) in the fitted g_2 for systematic variations in the MC.

	a_T	a_L	Q_T	b_T
p_T smearing $\pm 1\%$	-0.02	∓ 11	∓ 2.8	∓ 0.03
$p_T \pm 10\%$	∓ 0.2	± 3.8	± 1.4	∓ 0.2
$f_{iso} \pm 10\%$	∓ 0.3	∓ 1.7	∓ 0.59	∓ 0.3
$ \eta \pm 10\%$	± 0.4	± 11	± 3.2	± 0.4
ϕ smearing $\pm 10\%$	-0.01	0.00	0.00	-0.02
FSR $\pm 10\%$	∓ 0.4	∓ 0.96	∓ 0.52	∓ 0.4

Table 1 shows the shifts in the fitted g_2 for the +ve and -ve systematic variations. For each of the variations, the shift in the fitted g_2 is substantially smaller using a_T or b_T than Q_T , and larger using a_L . In fact the only variation to which a_T or b_T are more sensitive is the ϕ smearing, but for any realistic detector ϕ resolution, the shift in g_2 is negligible.

7.2 Statistical Sensitivity

Simply discarding information from a_L is not optimal in terms of the statistical sensitivity to the shape of the Q_T distribution (and thus also the value of g_2). As well as the basic observables, Q_T , a_T and a_L , the following ideas are

proposed as possible optimised combinations of a_T and a_L :

- A weighted quadrature sum of a_T and a_L with more weight (w) given to a_T :

$$Q_T^*(w) = \frac{1}{w^2} \sqrt{(w \cdot a_T)^2 + a_L^2} .$$
- A 2D fit to $\frac{d^2\sigma}{da_T da_L}$.

Table 2

The binning and 1σ statistical uncertainties for each of the g_2 fits, for a range of $\delta(1/p_T)$.

	Q_T	a_T	a_L	$Q_T^*(w = 5)$	$\frac{d^2\sigma}{da_T da_L}$	b_T
nbins	20	20	20	20	$20(a_T) \times 20(a_L)$	20
range (GeV)	0-30	0-20	0-20	0-30	0-20(a_T), 0-20(a_L)	0-20
$\delta(1/p_T)$ (GeV ⁻¹)	1σ statistical uncertainty (%)					
0.0000	1.4	2.2	2.4	1.9	1.4	2.2
0.0003	1.4	2.2	2.5	1.9	1.4	2.2
0.0010	1.8	2.2	3.6	1.9	1.6	2.2
0.0030	3.1	2.3	8.9	2.2	2.1	2.2

The binning and 1σ statistical uncertainties for each of the fits is presented in Table 2. Since the relative statistical sensitivity of each of the observables depends on the detector resolution, the fit is performed for different widths of Gaussian smearing. All of the fits use equal width bins. For “perfect” resolution, a fit to Q_T and the 2D fit have comparable statistical uncertainties. A fit to a_T or a_L alone is less statistically sensitive, as each contains information on only one component of the Q_T .

At larger $\delta(1/p_T)$, the sensitivity of a_L is completely washed out by the smearing. For $\delta(1/p_T) = 0.003$ GeV⁻¹, a_T alone gives better statistical precision than Q_T . Over the resolution range covered, $Q_T^*(w = 5)$ gives slightly better statistical precision than a_T alone. Note that no attempt has been made to optimize the weight in $Q_T^*(w = 5)$ as a function of resolution, and $w = 5$ is a somewhat arbitrary choice. Clearly, for “perfect” resolution, $w = 1$ is the only sensible choice. Once experimental systematic uncertainties are taken into account, a_T will need to be given more weight in any optimal combination of a_T and a_L .

7.3 Sensitivity to Small- x Broadening

The NP form factor (Eq. 1) required an alteration, to describe deep inelastic scattering (DIS) data involving initial state partons with $x < 10^{-3}$ [13]. Berge *et al.* [14] suggested that if this (so-called small- x broadening) was observed

at the Tevatron in an exclusive high $|y|$ sample of Z bosons, a broader Higgs (and W, Z) boson transverse momentum distribution could be expected at the LHC. The DØ Run II data on Q_T [4] disfavoured this modification, although given the large uncertainties, the data was not particularly sensitive to such broadening. Even without taking into account the reduced systematic uncertainties, the optimised fits (Q_T^* , $d^2\sigma/da_T da_L$) described earlier would be more sensitive to such effects. Once systematic uncertainties are taken into account, the sensitivity is further enhanced relative to the Q_T .

7.4 Azimuthal Correlation Between the Recoil and the Leptonic Decay

The example g_2 measurement presented would be sensitive to the description by the MC event generator(s) of the azimuthal correlation between the hadronic recoil and the leptonic decay. A measurement of $d^2\sigma/da_T da_L$ could be used to study this correlation.

8 Conclusions

Using MC simulations we demonstrate the potential benefits of decomposing the Q_T into two orthogonal components, a_T and a_L . A measurement of the a_T distribution would be substantially less sensitive to two of the dominant experimental systematic uncertainties reported in previous Q_T measurements: lepton p_T or E_T mis-measurement, and the Q_T dependence of the event selection efficiencies. A slightly different variable b_T is demonstrated to be similarly insensitive to these uncertainties. An optimal combination of a_T and a_L , giving more weight to a_T gives, for any realistic detector resolution, better statistical sensitivity to the shape of the region of low Q_T . Two possibilities are proposed: a weighted quadrature sum of a_T and a_L or a fit to $d^2\sigma/da_T da_L$.

A measurement of $d^2\sigma/da_T da_L$ could potentially probe the azimuthal correlation between the Z boson decay axis and the hadronic recoil. The partial differential cross sections; $d^2\sigma/da_T dQ$, $d^2\sigma/da_T dy$ and $d^3\sigma/da_T dQ dy$ could also be measured, taking advantage of the reduced systematic uncertainties on a_T compared with similar measurements of differential cross sections with respect to Q_T . Such distributions would be sensitive to small- x broadening effects.

References

- [1] J. Collins, D. Soper, G. Sterman, Nucl. Phys. B 250, 199-224 (1985).
- [2] F. Landry *et. al.*, Phys. Rev. D 67, 073016 (2003).
- [3] C. Balazs, C.P. Yuan, Phys. Rev. D 56, 5558-5583 (1997).
- [4] DØ Collaboration, Phys. Rev. L. 100, 102002 (2008).
- [5] DØ Collaboration, B. Abbott *et. al.*, Phys. Rev. D 61, 032004 (2000); DØ Collaboration, B. Abbott *et. al.*, Phys. Rev. L. 84, 2792 (2000).
- [6] OPAL collaboration, K. Ackerstaff *et. al.* Eur. Phys. J C4 47 (1998).
- [7] UA2 Collaboration, J. Alitti *et. al.* Z. Phys. C 47 523-531 (1990).
- [8] T. Sjöstrand *et. al.*, Comput. Phys. Commun. 135, 238 (2001).
- [9] DØ Collaboration, V.M. Abazov *et. al.*, Nucl. Inst. and Meth. A 565 465-537 (2006).
- [10] CDF Collaboration, CDF TDR, FERMILAB-Pub-96/390-E (1996).
- [11] ATLAS Collaboration, ATLAS TDR 14, CERN/LHCC 99-14 (1999).
- [12] CMS Collaboration, CMS TDR 8.1, CERN/LHCC 2006-001 (2006).
- [13] P. Nadolsky, D.R.Stump, C.P. Yuan, Phys. Rev. D 64, 114011 (2001).
- [14] S. Berge, P. Nadolsky, F. Olness, C.P. Yuan, Phys. Rev. D 72, 033015 (2005).
- [15] G.A. Ladinsky, C.P. Yuan, Phys. Rev. D 50, 4239 (1994).